Friction **2**(1): 40–46 (2014)
DOI 10.1007/s40544-014-0037-3 ISSN 2223-7690
RESEARCH ARTICLE

The nature of the frictional force at the macro-, micro-, and nano-scales

Esteban BROITMAN*
IFM, Linköping University, SE 58183, Sweden
Received: 23 June 2013 / Revised: 13 November 2013 / Accepted: 06 December 2013

Abstract: Nowadays it is accepted that the friction force is a combined effect arising from various phenomena: adhesive forces, capillary forces, contact elasticity, topography, surface chemistry, and generation of a third body, etc. Any of them can dominate depending on the experimental force and length scales of the study. Typical forces in macro-tribology are in the Newtons, while are reduced to milli-/micro-Newtons, and nano-Newtons in micro- and nano-tribology, respectively. In this paper, experimental friction results from fullerene like CN_x films and single-crystal Si at the three scales will be discussed. The complex and broad variety of processes and phenomena connected with the dry friction coefficient at the macro-, micro-, and nano-scale point of view will be highlighted.

Keywords: macrotribology; microtribology; nanotribology; carbon nitride; silicon

1 Introduction

The understanding of the nature of the frictional force has evolved since Amontons' work in 1699 [1]. Nowadays it is accepted that the force is a combined effect arising from various phenomena: adhesive forces, capillary forces, contact elasticity, topography, surface chemistry, and generation of a third body, etc. Any of these effects can dominate depending on the experimental force and length scales of the given sliding system.

In *macrotribology*, the dry interaction between two surfaces in contact is governed by Amontons' laws [1] stating that the friction force F_{fr} is:

$$F_{fr} = \mu N \quad (1)$$

where μ is the coefficient of friction and N is the normal contact force. The macrotribology approximates the geometrical contact area of two bodies to the real contact area on the atomic scale: F_{fr} depends only on N (reaction pair of the applied load), and is independent of the surface area in contact. Also, at this length scale, friction is generally accompanied by elastic and plastic deformation, wear, and even fracture on the contact surfaces.

In *microtribology*, the dry contact between two surfaces takes into consideration the real microscopic roughness through the interaction of asperities. In 1954, Bowden and Tabor proposed that friction was originated from the plastic deformation of interlocking spherical asperities [2]. As a result, the frictional force was proportional to the real contact area defined by the junctions of asperities formed by contact pressure and adhesion. Considering the deformation of a single asperity according to Hertz contact theory, they concluded that the friction force was:

$$F_{fr} = S\pi(RN / K)^{2/3} \quad (2)$$

where S is the shear stress of the asperity junction, R is the asperities reduced radii of curvature, and K is the reduced Young's moduli of the two interacting asperities. While in Amonton's macrotribology the friction force is proportional to N, in Bowden and Tabor's microtribology F_{fr} is proportional to $N^{2/3}$.

* Corresponding author: Esteban BROITMAN.
E-mail: esbro@ifm.liu.se
A preliminary version of this work was presented at the 3rd International Symposium on Tribology of IFToMM, Luleå, Sweden, 2013.

Adhering asperities are formed as normal load is applied, and friction is caused during relative motion by loss of energy due to junctions break at or near the contact interface. This seminal model sparked further theoretical and experimental research in terms of single- and multi-asperity contact mechanics, and the linking of adhesion and friction concepts.

In *nanotribology*, the dry contact between two surfaces considers the interaction at atomic scale. In 1929, Tomlinson proposed an atomic friction model based on the assumption that the surface was atomically smooth without any asperity [3]. However, since atoms were modeled as spheres, the surface topography consisted of protrusions separated by the lattice constant. When the counter surface slid on top, the interaction could be represented by a spring-like interaction that undergoes stretching and contraction as the atoms slide against each other. In 1939, the Frenkel-Kontorova model proposes a 1-dimensional interaction between the substrate atoms with sinusoidal potential and a chain of surface atoms linked by harmonic springs and a periodic potential force applied to the atoms. The model was further discussed and extended by other authors, until it reaches the form of what is known nowadays as the FKT (Frenkel-Kontorova-Tomlinson) model. This model also provides the possibility of a wearless frictional interaction, and the commensurability on the friction behavior [4]. During the last decade, with the advancement of computational capability, the use of computer simulation to investigate atomic-scale interactions has been steadily increasing. Since continuum mechanics is not valid at the atomic scale, analytical methods such as Molecular Dynamics, Monte Carlo, and *Ab-initio* calculations have been used, as it has recently reviewed by Kim et al. [5].

There is also other important factor responsible for the difference in the coefficients of friction at the macro-, micro- and nano-scale. The sliding of materials in contact often involves wear, i.e., the generation and transfer of material from one surface to the other. This material, referred to sometimes as the "*third body*", influences the transient behavior of the sliding contact and can completely dominate the steady-state sliding behavior of many interfaces, especially for low friction coatings [6]. At macro- and micro-scale, transfer films are formed during initial sliding, and these films determine the long-term frictional behavior of the interface [7]. At nanoscale third-bodies can also have a large impact on the contact properties; molecular dynamics simulations indicate that molecular intermediate species in asperity contacts have a dramatic effect on friction [8].

In this paper, similarities and differences on dry friction experimental results at macro-, micro-, and nano-scales will be reviewed and discussed. Results from fullerene-like CN_x coatings with friction coefficients μ ranging from 0.05 to 0.30 when measured on wet and dry conditions by reciprocating tests will be discussed in terms of macro- and nano-scale effects. The dependence of the friction values with the measurement scale on single-crystal Si (001) will be analyzed. A complex and broad variety of friction phenomena in the macro- micro and nano-tribology worlds will be discused.

2 Friction of CN_X films at macro- and nano-scale

Amorphous carbon-based coatings have found many applications as protective coatings and solid lubricants. By tuning the C sp^3-to-sp^2 bonding ratio and by alloying the carbon with other elements, the properties of the coatings can be tailored. Recently, we have shown that it is possible to incorporate fullerene-like features to a solid matrix of C and N. The resulting so called fullerene-like (FL) compound consists of sp^2-coordinated graphitic basal planes that are buckled due to the presence of pentagons and cross-linked at sp^3-hybridized C sites, both of which are caused by structural incorporation of nitrogen. This fullerene-like carbon nitride (FL-CN_x), which possesses a superior resiliency to mechanical deformation due to its unique superelasticity, shows potential as protective top coat on computer hard disks and biocompatible coatings on orthopedic implants [9, 10].

2.1 CN_x friction at the macroscale

Macro-tribological sliding friction tests were performed using a reciprocating–sliding tribometer. The reciprocation stage was designed to fit directly underneath the

optics of a microscope, enabling *in situ* optical/video imaging and/or Raman spectroscopy of the sliding contact region through a transparent hemisphere [7]. A 6.35 mm diameter sapphire hemisphere was used with a load of 6.4 N. Friction tests were performed in either dry or ambient (50% RH) air at room temperature. Each test was run between 6 and 5,000 cycles over track lengths of 6 mm for the first 300 cycles and then cut back to 4 mm for the remaining cycles at a sliding speed of 4 mm·s^{-1}[7].

Figure 1 presents the hardness and density, as well as the friction and wear rates after 300 cycles in dry air (squares) and 50% relative humidity (circles) environment for FL-CN$_x$ films grown at 10, 25, and 40 V bias voltage [7]. It was found that an increase in bias voltage produces an increase in hardness (H) and density (ρ) of the films. In dry air, wear rates were higher than in humid environment for all coatings. We can also observe that the hardness and density variation of the coatings correlates with the wear rate and friction coefficient: at higher hardness and higher densities, the wear rate and friction coefficient decrease. *In situ* analysis showed that a thick transfer film formed slowly, which caused considerable wear of the coating (initially) but isolated the hemisphere from the track and provided a steady friction coefficient.

In humid environments, the wear rate increases with the hardness and density of the coating, while the friction coefficient decreases. *In situ* analysis of the sliding contact suggests that humidity in the air

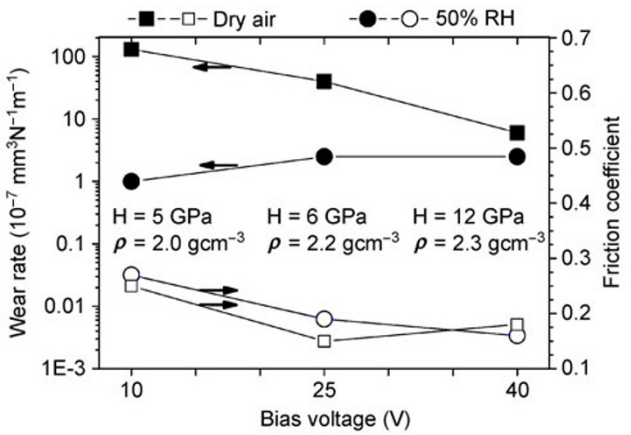

Fig. 1 Friction coefficient and wear rate of carbon-based coatings deposited at different bias voltages, and measured at dry air and 50% RH (Reproduced with permission from Ref. [7]. Copyright Elsevier, 2008).

protected the coating from wear and allowed a lower friction. *In situ* videos recorded during the experiments showed interfacial sliding between a barely visible transfer film and the wear track, which occurred throughout the test and maintained steady-state friction coefficients. This separation of the wear track from the ball, supposedly by the influence of a humidity-modified film, would also account for the low wear rates. We have previously noticed [11] a significant change of the resistivity of CN$_x$ films during exposure to ambient air. It is possible that reactions with absorbed water on the film surface saturate reactive surface sites, which in turn alters the tribo-chemistry of the surface [7]. The drop in the friction coefficient of FL–CN$_x$ coatings with increasing bias, corresponding to decreased number of nucleation sites, suggests that water was adsorbed (as OH$^+$) at these sites and promoted different friction layers. The discrepancies were accounted for with *in situ* visualization which showed that wear life and friction behavior were controlled by transfer films and not by mechanical properties [7].

2.2 CN$_x$ nanoscale computer simulations

The behavior shown in Section 2.1 for FL-CN$_x$ thin films in humid environment have been further studied at the nanoscale. Figure 2 shows the adsorption of water versus the water vapor pressure for different carbon-based films: amorphous carbon (a-C), amorphous carbon nitride (a-CN$_x$), and fullerene-like carbon nitride [12]. All carbon-based films show a similar dependence of water coverage on the H_2O vapor pressure. There are, however, differences in the amounts of the adsorbed water: (i) FL-CN$_x$ shows the lower adsorption rate. Taking into consideration one monolayer coverage is roughly 30 ng/cm^2 and that at room temperature 13.3 × 10^2 Pa of H_2O vapor pressure is equivalent to 50% RH [12], these films adsorb less than 2 ML at that pressure; (ii) a-CN$_x$ has adsorbed roughly 2–3 times more water than FL-CN$_x$. (iii) Finally, a-C adsorbs more than 14 times the amount adsorbed by FL-CN$_x$. Water absorption in carbon-based coatings can be influenced by many factors like dangling bonds, surface contaminants, and top dead layers of low density carbon, etc. Electro-spin resonance measurements were done in our films [12].

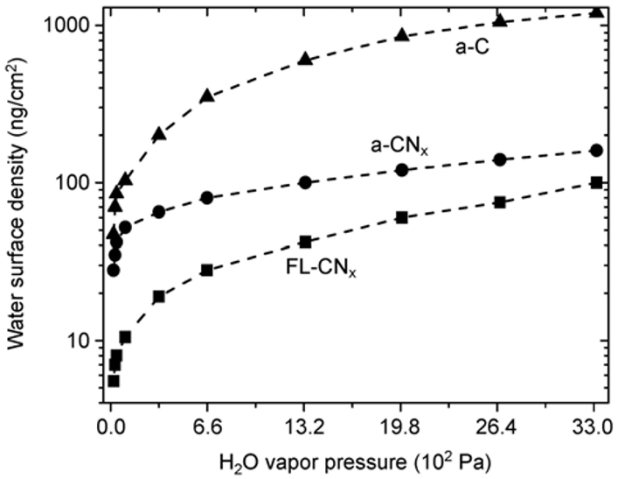

Fig. 2 Water adsorption as a function of water vapour pressure for different carbon-based coatings. (Reproduced with permission from Ref. [12]. Copyright Elsevier, 2008)

In order to understand the water adsorption at the nanoscale, finite model systems simulating a-C, a-CN_x, as well as systems in which N is incorporated in sp^2-hybridized graphene sheets (to represent FL-CN_x) were recently considered [12]. The study involved both geometry optimizations and cohesive energy (E_{coh}) calculations performed within the DFT framework in its generalized gradient approximation (GGA). Differences in cohesive energies $|\Delta E_{coh}|$ for the possible structures were determined by an optimization strategy presented in Ref. [12].

The results from the calculations have shown that in a-C films the energy cost for a dangling bond is by ~0.1 eV lower than in a-CN_x and by ~0.3–0.9 eV (depending on the type of defect) lower than in FL-CN_x. Thus in a-C, the likeliness of dangling bonds is considerably higher than in FL-CN_x, and still somehow higher than in a-CN_x [12], confirming our experimental results of Fig. 2. In the case of the fullerene-like films deposited at different bias voltage (Fig. 1), the calculations also confirm that films with the lower friction coefficient have a lower number of dangling bonds.

3 Macro-, micro-, and nano-tribology of Si (100)

Microelectromechanical systems (MEMS), based on semiconductor fabrication techniques, have allowed the creation of a wide range of miniaturized mechanical devices including gear assemblies, mirror arrays and accelerometers. The practical use of MEMS, however, is limited in many applications; one of the principal problems is that friction and wear limit the operating lifetimes of all mechanical systems and these issues are, if anything, even more problematic in MEMS than in macroscopic mechanical systems [13].

The most common MEMS material is Si which, in its native state, is coated with a thin film of SiO_2. The mechanical properties and surface chemistry of Si and SiO_2 are completely different from those of ferrous alloys or other metals. Although a great deal is known about the surface chemistry of Si because of its importance in the semiconductor industry, the relevance of that body of knowledge to Si tribology is not clear. What is interesting is that, by comparison with metallic surfaces, there has been comparatively little study of the fundamental tribological properties of Si surfaces, and most of them give a wide spread of friction coefficients in the range 0.005 to 1 [13, 14].

Figures 3, 4, and 5 illustrate the dry friction coefficient of a single-crystal Si (100) bulk sample that we have measured with three different tribo-apparatus. At first glance, it seems that μ depends on the scale of the measurement method; a careful analysis of the experiment conditions enlights the reason for the differences.

Figure 3 is the macro-scale measurement of the friction coefficient in a ball-on-disk tribometer (VTT) [15]. The ball was a steal ball–bearing of 6 mm diameter

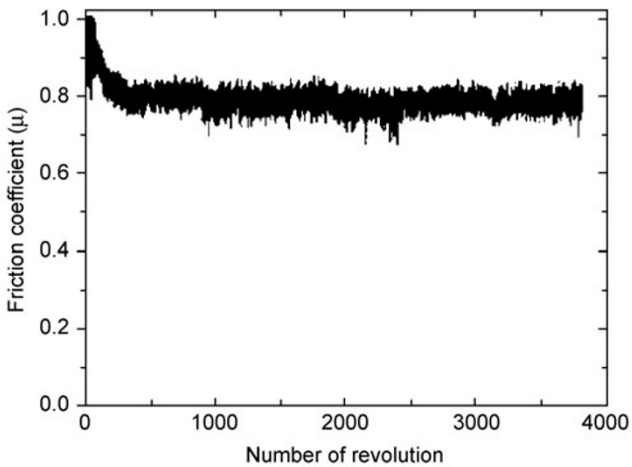

Fig. 3 Macroscale friction coefficient of single-crystal Si (001) as a function of number of revolution (Reproduced with permission from Ref. [15]. Copyright Elsevier, 2001).

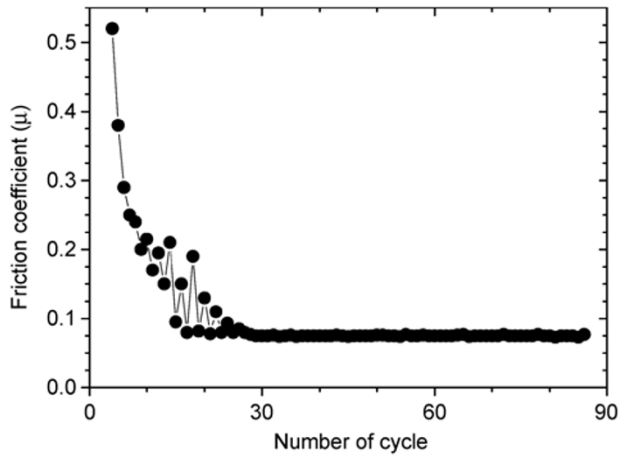

Fig. 4 Microscale friction coefficient of single-crystal Si (001) as a function of number of revolution.

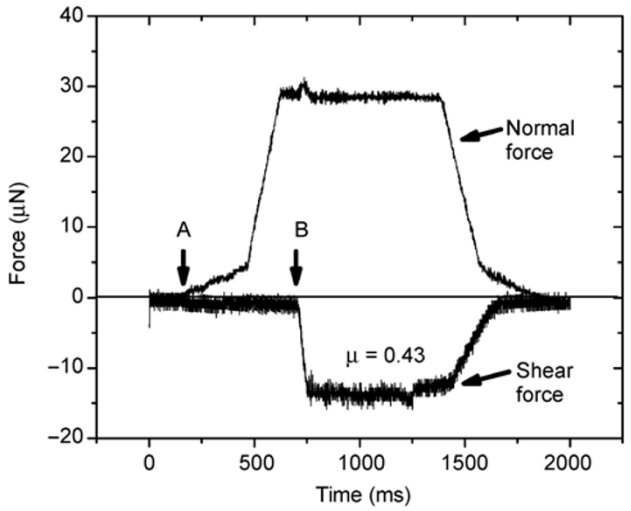

Fig. 5 Nanoscale friction measurement of single-crystal Si(001).

with an applied load of 2 N, resulting in an initial contact pressure, according to Hertz, of about 0.64 GPa. The rotary speed was 180 rpm, the track diameter was 6 mm, and the test duration was 20 min. The test, performed in ambient atmosphere, shows at the beginning that μ increases in 10 revolutions up to ~1, but then it starts to decrease to reach a steady state value of ~0.75 after 250 revolutions. Optical microscopy revealed a severely damaged wear track and the presence of wear debris.

Figure 4 is the micro-scale friction coefficient measured with a Triboindenter TI 950 reciprocal test (Hysitron). The conical diamond probe had a curvature radius of ~5 μm and an applied load of 0.5 μN, resulting in an initial contact pressure of ~ 3.9 GPa (according to Hertz). The track had a stroke of 10 μm, and each cycle was done in 20 seconds. The test, performed in ambient conditions, shows also at the beginning a peak friction coefficient μ ~ 0.5 which decreases to reach a steady state value of μ ~ 0.075 after 29 cycles. Surface probe microscopy has also shown a wear track and the presence wear debris.

Finally, Fig. 5 is the nano-scale characterization of Si measured with a UHV tribometer working as a surface probe apparatus. The original substrate support of the instrument was adapted to hold two ultra-thin (10 μm thick) single crystalline foils of Si(100) mounted in cross-cylinder geometry (Fig. 6). They were sufficiently flexible that, when brought into contact, they deformed elastically by bending rather than deforming plastically. Normal and shear forces between at the Si(100)/Si(100) interface during one single-pass sliding were measured, and at a peak force of 30 μN the friction coefficient resulted μ ~ 0.43.

It is clearly observed that friction values are scale dependent. If we consider only the starting friction value, μ goes from ~1 at the macroscale, to ~0.5 at the microscale, and to ~0.4 at the nanoscale. In the steady state, μ goes from ~0.75 at the macroscale to ~0.075 at the microscale. It is well known that phase transformations and amorphization can occur in silicon under contact loading, and new formed phases would have different frictional properties. However, that possibility can be discarded because under ambient conditions, the first Si transition occurs in the pressure range of 9 to 16 GPa [1, 16], which is higher than the contact pressures used in our experiments. According to Bhushan [17], we can find at least four possible differences in the operating conditions responsible for the friction differences in our

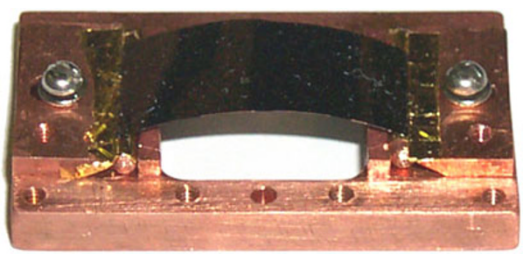

Fig. 6 The sample mounting frame of the UHV tribometer with a piece of Si(100) foil bent to form a cylindrical section. The foil is elastic and when released is flat. The frame is roughly 2.5 cm in width.

experiments. First, the contact stresses at the contact; the average contact stresses in the macrocontact of the 6 mm diameter ball will be lower than for the microcontacts of the 5 μm diameter contact of the Triboindenter probe, however, at the macroscale a large number of asperities come into contact which go through some plastic deformation. Second, the smaller apparent area of contact reduces the number of particles trapped at the interface, and thus minimizes the third-body plowing contribution to the friction force at the microscale. Third, the Triboindenter has a relatively sharp tip with nanoasperities, whereas asperities coming in contact at the macroscale test range from nanoaspereties to much larger asperities which may be responsible for larger values of friction force on macroscale. As a fourth and final difference, when measuring in the nanoscale experiment with small contact area and very low loads, the lack of plastic deformation reduces the degree of wear and friction.

4 Concluding remarks

In this paper, we have compared the friction coefficient of carbon-based coatings and bulk Si. At the macroscale, during dry environment tests, the friction and wear of FL-CN_x coatings are dominated by the presence of third body. On the other hand, on humid environments, the friction and wear of FL-CN_x coatings are influenced by tribochemical reactions. Nanoscale simulations have confirmed that the tribochemistry can be linked to the amount of dangling bonds on the surface of CN_x. Finally, experiments with bulk Si have shown that the friction is scale dependent. All the discussed results illustrate the complex and broad variety of processes and phenomena connected with the dry friction coefficient at the macro-, micro-, and nano-scale point of view.

Acknowledgements

The author acknowledges L. Hultman, G. K. Gueorguiev, H. Sjöström, N. Hellgren, J. Neidhardt, A. Furlan, I. Singer, and A. J. Gellman for valuable discussions. The support of the Swedish Government Strategic Research Area in Materials Science on Functional Materials at Linköping University (Faculty Grant SFO-Mat-LiU # 2009-00971) is highly appreciated.

References

[1] Amontons G. De la résistance causée dans les machines. *Mémoires de l'Académie Royale A*: 257−282 (1699)

[2] Bowden E, Tabor D. *The Friction and Lubrication of Solids*. London: Oxford University Press, 1954.

[3] Tomlinson G. A molecular theory of friction. *Philos Mag* **46**: 905−939 (1929)

[4] Braun O, Kivshar Y. Nonlinear dynamics of the Frenkel-Kontorova model. *Phys Rep* **306**: 1−108 (1998)

[5] Kim H-J, Kim D-E. Nano-scale friction: A review. *Int J Precis Eng Manuf* **10**(2): 141−151 (2009)

[6] Singer I. How third-body processes affect friction and wear. *MRS Bulletin* **23**(6): 37–40 (1998)

[7] Neidhardt J, Hultman L, Broitman E, Scharf T W, Singer I L. Structural, mechanical and tribological behavior of fullerene-like and amorphous carbon nitride coatings. *Diam Relat Mater* **13**: 1882−1888 (2004)

[8] Enachescu M. Nanoscale effects of friction, adhesion and electrical conduction in AFM experiments. In *Atomic Force Microscopy—Imaging, Measuring and Manipulating Surfaces at the Atomic Scale*. Intechopen.com, 2012: 99−146.

[9] Broitman E, Neidhart J, Hultman L. Fullerene-like carbon nitride: A new carbon-based tribological coating. In *Tribology of Diamond-like Carbon Films*. New York: Springer, 2007: 620−653.

[10] Broitman E, Furlan A, Gueorguiev G K, Czigány Z, Högberg H, Hultman L. Structural and mechanical properties of CN_x and CP_x thin solid films. *Key Eng Mater* **488−489**: 581−584 (2012)

[11] Broitman E, Hellgren N, Neidhardt J, Brunell I, Hultman L. Electrical properties of carbon nitride thin films: Role of morphology and hydrogen content. *J Electron Mater* **31**(9): L11-L15 (2002)

[12] Broitman E, Gueorguiev G K, Furlan A, Son N T, Gellman A J, Stafström S, Hultman L. Water adsorption on fullerene-like carbon nitride overcoats. *Thin Solid Films* **517**: 1106−1110 (2008)

[13] Williams J, Le H. Tribology and MEMS. *J Phys D: Appl Phys* **39**: R201−R214 (2006)
[14] Maboudian R, Carraro C. Surface chemistry and tribology of MEMS. *Annu Rev Phys Chem* **55**: 35−54 (2004)
[15] Broitman E, Hellgren N, Wänstrand O, Johansson M P, Berlind T, Sjöström H, Sundgren J-E, Larsson M, Hultman L. Mechanical and tribological properties of CN_x films deposited by reactive magnetron sputtering. *Wear* **248**: 55−64 (2001)
[16] Domnich V, Gogotsi Y. Phase transformations in silicon under contact loading. *Rev Adv Mater Sci* **3**: 1−36 (2002)
[17] Bhushan B. Nanotribology and nano-mechanics. *Wear* **259**: 1507−1531 (2005)

Esteban BROITMAN. He received his PhD degree in physics from the University of Buenos Aires, Argentina, in 1997. He has been doing research and teaching at the University of Buenos Aires (Argentina), The College of William and Mary (USA), and Carnegie Mellon University (USA). He is currently a guest professor at Linköping University (Sweden). His research activities focus on the physical properties of thin films deposited by vapor-phase deposition and sol-gel methods, like microstructure evolution, mechanical and tribological properties. His particular interest is in the area of thin film micro- and nano-tribology.